ISSN: 0976 - 2965
IJBET (2010), 1(1):30-36

# Finite Element Analysis of Vascular Tissue during Stent Placement: Estimation of Injury

V. V. Shukla[1*], P. M. Padole[1]

1 Department of Mechanical Engineering, Visvesvaraya National Institute of Technology, Nagpur, M.S., India - 440011,
vivshukla@yahoo.com

**ABSTRACT**:

Several previous studies on stents and stenting technology have investigated various design and behavioral response parameters of stent and /or balloon. However, the ultimate physiological objective still remains to safeguard the soft tissue and maintain the patent blood flow by reducing the extent of stenosis. Therefore to envisage the effect of stent expansion on to the arterial tissue, it is necessary to analyze the contact physics of Balloon Stent Plaque and Artery (BSPA) combined system. Based on which one can quantify and characterize the stresses on arterial tissue. Most of the previous studies have ignored the presence of plaque and artery. In this investigation, the authors have defined 3 contact pairs on 2 non-linear materials (Balloon & Stent) and 2 linear materials (Plaque & Artery) using advanced Finite Element Analysis Techniques. The vascular injury has been hypothesized in terms of stresses using contact mechanics. The results are in good agreement with available but limited previous studies. It can be concluded that contact stress analysis of the mechanical interactive behaviour of the Balloon-Stent-Plaque and Artery collectively; is a decisive procedure for the design and application of similar vascular implants.

**Keywords**: Balloon-Stent-Plaque-Artery (BSPA), Finite Element Analysis (FEA), Contact Mechanics

## INTRODUCTION

A sedentary lifestyle, rich diet, lack of exercise smoking etc. leads to an increase in blocked blood vessels, hypertension and strokes. A material called plaque builds up on the inner wall of arteries. The plaque makes the artery wall narrow and hard. Stenosis is the narrowing of the blood vessel due to deposition of atherosclerotic plaque on the inner surface of the vessel wall. Stenosis may present with hypertension, recurrent episodes of congestive heart failure and flash pulmonary edema or may be discovered incidentally during an imaging procedure for some other reason. The high blood pressure that is sometimes associated with stenosis may be the first sign that it is present, particularly if the hypertension is not responding to standard treatment. It is vital to develop effective treatments that prolong the life of a patient. Prompt diagnosis and timely intervention done by a skilled vascular surgeon can significantly decrease target organ damage and potentially cure high blood pressure due to stenotic arteries. Management of stenosis consists of three possible strategies: medical management, surgical management or percutaneous therapy with balloon angioplasty and stent implantation. If stenosis is detected, the vascular surgeon will determine which of the method of repair; viz. Angioplasty, stent placement or arterial Bypass would be the most appropriate and beneficial for each patient's unique situation. Stenting has replaced surgical revascularization for most patients with atherosclerotic disease who meet the criteria for intervention. Cardiovascular surgeons expand narrowed arteries and control blood pressure (BP) so that patients live longer and have no strokes.

Stent deployment is currently the preferred vascular interventional procedure to treat stenosis [1]. Stenting has also benefited individuals with diabetes, who have increased risk of stenosis. In addition, up to two-thirds of diabetic individuals develop life-threatening heart or blood vessel disease. Stenting has compared favorably to balloon angioplasty in reducing the incidence of heart attack and need for repeat artery-widening procedures. Yet, restenosis, artery collapses, stent migration and positioning complexity are clinically exigent issues. In-stent restenosis (ISR) still remains an obsession to Cardiologists [2]. Vascular injury can be hypothesized as the stimulus for the formation of occlusive intimal hyperplasia and eventual restenosis [3]. In fact, vascular injury caused to a vessel by the implantation of a stent, whether defined by the depth of penetration of the stent wires or by an aggressiveness score, has consistently been found to determine the degree of restenosis [4]. Factors influencing the restenosis process include the degree of damaged endothelial cells and the depth of the injury [5], the design of the stent, the type of stent expansion (self or balloon-expandable) [6]. The clinical problem associated with stent procedures is the high restenosis rates [7]. To avoid these problems, stents are usually over deployed at pressures beyond what would be considered optimal [8]. Excessive expansion of a stent during deployment may also cause extensive vessel damage, and recent data indicate that shear stress mediates the rate of smooth muscle cell migration after

injury [9]. Vascular damage produced by an over-expanded stent may predispose this vascular segment to the development of neointimal hyperplasia by adversely affecting distributions of wall shear stress. Basically the immune cells which adhere to the vessel walls, scavenge cholesterol from blood due to inflammatory signals and then it develop a new type of cell called foam cells thus causing formation of plaques. The focal vascular trauma imposed by the stent struts, the stress and strain environments around the expanded stent and the existence of a foreign material in the injured artery may trigger molecular mechanisms, leading to inflammation, granulation, and extracellular matrix production leading to reclosure needing further intervention. The most important mechanism that leads to restenosis is the inflammatory response, which induces a tissue proliferation (neointimal hyperplasia) around the angioplasty site [10, 11]. Another difficulty during stent deployment is stent positioning. It is believed that the stent design may affect the neointimal growth. Better surface and cut quality can prevent the activation process of thrombosis and show a decrease in neointimal hyperplasia as well as improve the healing efficiency. During stenting it is common for large deformations of the vessel tissues to occur, which can lead to arterial overstretching and eventual vessel injury [12, 13]. Despite the early promising results, reduction of the restenosis rates to less than 10%, the mechanical vascular injury by stent insertion is not eliminated with the recently developed pharmacological coatings.

Nowadays, computational structural analyses have emerged as an important tool to investigate the mechanical response to stent placement inside arterial walls [14-18] by imposing pressure to the internal stent struts [19-21]. Many of the previous studies, discards the balloon from the analyses and simulates the interaction between the balloon and the stent by a (uniform) pressure distribution on the inner surface of the stent [22-24]. The stent-free expansion shows considerable discrepancy between numerical results and reality when the presence of the balloon is discarded [25].

Hemodynamic factors such as velocity gradients, shear stresses etc. are believed to affect a number of cardiovascular diseases including stenosis and aneurysms. Since resolving phenomenon in living body is beyond the capabilities of in vivo measurement techniques, computer modeling is expected to play an important role in gaining better understanding of the relationship between cardiovascular disease and hemodynamic factors. When physical test methods are difficult (or even impossible), computational models may sometimes be the only alternative. In Biomechanics, Finite Element Analysis (FEA) and computational Fluid Dynamics (CFD) are increasingly used to perform strength analysis, system response studies and design optimization of implants without the need for time- and cost-intensive prototyping. The rapidly improving computer performance enables a low-cost simulation of complex components or composite structures. Different medical and technical demands on the modeling or material laws can be examined by FEA.

The objective of this study is to numerically assess the damage or superficial injury caused to the plaque and/or artery during stent deployment using 3-D Nonlinear Finite Element Analysis (NFEA). The vascular injury or damage has been hypothesized in terms of stresses, strains and displacement.

## MATERIALS AND METHODS

A symmetrical nonlinear finite element simulation was performed to analyze interaction between the Balloon, the slotted tube Stent, Plaque and the Artery (BSPA) during stent deployment. The analysis was performed using ANSYS®, V 11.0, as a pre and post processor. The coexisting presence of two linear materials (Plaque and artery) and two nonlinear materials (Balloon and stent) frames the 3-D contact problems with deformable bodies. Hence explicit scheme was chosen to run the analyses. A typical Palmaz-Schatz type stent consists of periodic structures along both the longitudinal and circumferential directions. The displacements and stresses over the stent, the plaque and the artery were computed and analyzed. The care was taken during modeling and meshing to ensure the orientation of element shell normal towards each other. Total of 45110 nodes and 27930 elements were created.

Due to the circumferential symmetry, only one-eighth of model geometry is necessary for analysis. The model geometry represents 64% stenosis. Figure 1 shows the combined BSPA assembly model. Figure 1(a) is obtained by reflecting the basic model about the planes of symmetry. Figure 1(b) shows the slotted tube stent model. The lengths of BSPA are 11, 10, 8 and 12 mm respectively. The inner diameters of BSPA are 2.5, 2.8, 3.2 and 4.4 mm respectively. The thicknesses of the BSPA are 0.15, 0.10, 0.60 and 0.60 mm respectively.

Finite element model with hyper elastic material properties were used for balloon. Two parameter hyperelastic Mooney–Rivlin model is used to represent the hyperelastic material of balloon with $C_{10}$ = 1.06881 MPa and $C_{01}$ = 0.710918 MPa. The material of the stent is assumed to be stainless steel 316L described as a bilinear isotropic elastoplastic model with Young's modulus equal to 201 GPa, the tangent modulus 1000 MPa, Poisson's ratio 0.3 and yield strength 215 MPa.

ISSN: 0976 - 2965
IJBET (2009), 1(1):30-36

Poisson's ratio was assumed to be 0.45 for balloon. For representing material of plaque and artery (soft tissue), Young's modulus 2.5 MPa and 1.25 MPa and Poisson's ratio of 0.45 and 0.49 was assigned respectively. Coefficient of friction 0.015 was assigned between each of the pairs to cope with the non-convergence difficulty. Densities of 1.07e-6, 7.8e-6 Kg/$m^3$ for Balloon and Stent are considered respectively and1.12e-6 Kg/$m^3$ for both Plaque and Artery respectively

The type of elements used for meshing stent geometry is solid 187 and solid 185 for Balloon, Plaque and Artery, as shown in Figure 1(c). TARGET 170 and CONTA 174 elements are automatically created in ANSYS once user defines the contact pairs between B-S, B-P, S-P and S-A using automated contact wizard. The number of nodes and elements for BSPA are: B (N3663, E2200), S (N9356, E4072), P (N15158, E4884) and A (N11011, E8640). The pair wise (Contact174: Target170) elements for respective contact pairs between B-S (1146:1146), B-P (100:1008), S-P (1100:1008) and between S-A (1146:480).

In order to verify the accuracy of the mesh density used in the analyses, a mesh sensitivity study was performed on all of the BSPA system. The adaptive meshing incorporated into the simulations resulted in an increase in the number of elements and nodes defining the hyperelastic artery and plaque materials in stenting deployment simulations. A surface to surface contact algorithm (Augmented Lagrange method) with contact detection on Gauss points was set. The implicit contact analysis was solved using sparse solver. Normal penalty stiffness of 0.1, penetration tolerance of 1 and unsymmetrical stiffness matrix for all the four deformable-deformable pairs was used. The details of other setting are shown in Table 1, where BO is Balloon outer surface, SI-Stent Inner surface, SO-Stent Outer, PI-Plaque Inner and AI-Artery Inner surfaces. Both the distal ends of balloon and artery were fully constrained and expansion in radial direction was allowed. Whereas stent and plaque had free boundary conditions and were allowed to move in any direction.

Symmetric boundary conditions were imposed on the symmetric planes of Balloon-Stent-Plaque-Artery system. The stent is expanded by applying a linearly increasing pressure of 1 MPa on the inner surface of the balloon. Pressure load provided the force which causes the dilation of the Balloon and thereby the expansion of the stent. The expansion of the stent produces the displacement of the vascular tissues. The displacements and stresses over the stent, the vascular tissues were computed and analyzed.

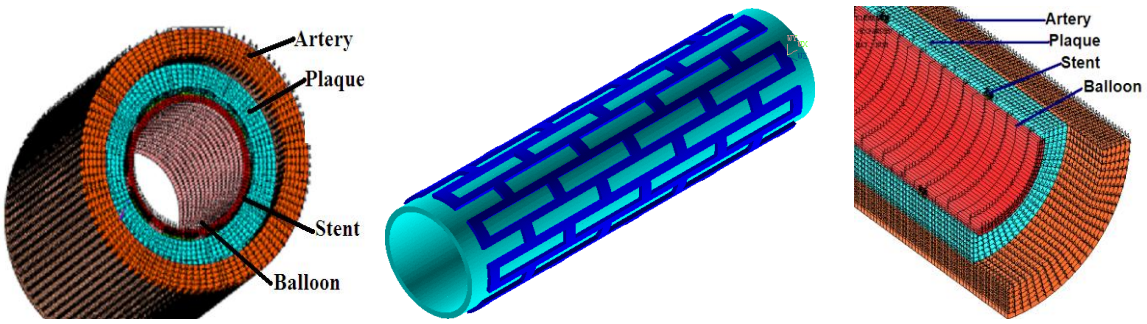


(a) (b) (c)

Figure 1. (a) Complete BSPA model (b) Balloon-Stent assembly (c) FE mesh of BSPA for 1/8$^{th}$ section model

Table 1. Details of the Contact pair defined and settings used for the analysis.

| Contact pair Number | Behaviour of contact surface | Initial penetration | Automatic contact adjustments | Resulting stiffness (N/mm) | Average contact surface length (mm) | Average contact surface depth (mm) |
|---|---|---|---|---|---|---|
| 1 (BO-SI) | No separation | Include everything | Reduce penetration | 292.82 | 0.106 | 0.73 |
| 2 (BO-PI) | Standard | Exclude everything | Reduce penetration | 8.8846 | 0.106 | 0.073 |
| 3 (SO-PI) | Bonded | Include everything | Close gap | 7.2824 | 0.102 | 0.089 |
| 4 (SO-AI) | Standard | Exclude everything | No adjustment | 2.9197 | 0.102 | 0.08 |

ISSN: 0976 - 2965
IJBET (2009), 1(1):30-36

## RESULTS AND DISCUSSION

Balloon-plaque, stent-plaque and stent-artery interactions during stent deployment create vascular injury. The acute contact of stent with plaque tissue causes intimal tissue proliferation. In order to determine the value of maximum radial displacement, the balloon is inflated until the onset of plastic deformation of stent is observed and the ultimate tensile strength of the stent material is reached. Maximum radial displacements for each component of BSPA system are observed to be 0.68, 0.68, 0.29 and 0.20 mm respectively, at maximum balloon inflation pressure of 10 atmospheres.

Figure 2 (a) shows the displacements (on Y-axis) of BSPA due to balloon inflation pressure in atmosphere (on X-axis) stent expansion. It can be seen that the radial displacement of artery tissue is least compared to BSP. Also the distal ends of balloon expand (0.68 mm) more than that of proximal portion (0.29 mm) due to lesser resistance to expansion. From Figure 2 (b), it is observed that strain produced in the stent material is significantly larger than other materials. Maximum total mechanical strains for each of BSPA are found to be 0.79, 0.13, 0.33 and 0.14 respectively. For the stent, maximum equivalent stresses are used for the direct comparison with ultimate tensile strength of the material. The distal ends of balloon expand more to that of proximal portion due to lesser resistance to expansion. The balloon under uniform pressure begins to expand at both ends because of the differences in material properties between the balloon and the stent; additionally due to resistance from the stent itself. When the force required for further expansion of balloon exceeds the resistant force from the stent, expansion of stent takes place. Similar conditions (flaring of distal ends) are observed in the response of stent material; this is basically due to cantilever type of strut arrangements at the distal stent ends. During the inflation process the proximal and distal ends of the expanding balloon, inflates first and causes the overlying stent to open non-uniformly. The displacement of free end of cantilever is always more to that of fixed ends and hence the well known dogbonning effect is observed in expanded stent. The displacement of distal ends is found to be more to that of proximal ends; this indicates well known dogbonning effect (20.6%). The maximum stress in the two parameter hyperelastic balloon is found to be 7.97 MPa as shown in figure 3 (a). The stent stress closely resembles the bi-linear stress–strain relationship of the material and is maximum 320 MPa at balloon pressure of 1.0 MPA. The bilinear nature of the stent material can be observed with a few inflation pressure pivots, which indicates a reliable solution. As the pressure increases, the reaction force of the stent is no longer able to hold the balloon back to its original state. The centre of the slotted tube stent opens with increasing pressure and causes a contraction along its axial length (foreshortening). The expanding and sliding stent-struts press against the plaque against the arterial wall.

It can be seen from the figure 3 (b) that the highly stressed areas are localized in the corners of the slots irrespectively of the design structure of the struts. Major stress was also found localized in the middle of the slots. With the assumed material model for plaque and artery the distribution of Von-Mises stresses on plaque tissue (harder) and artery wall (soft tissue) are shown in Figure 3 (c) & Figure 3 (d) respectively. Further, the impression stamps of the stent cells are observed in the vascular wall.

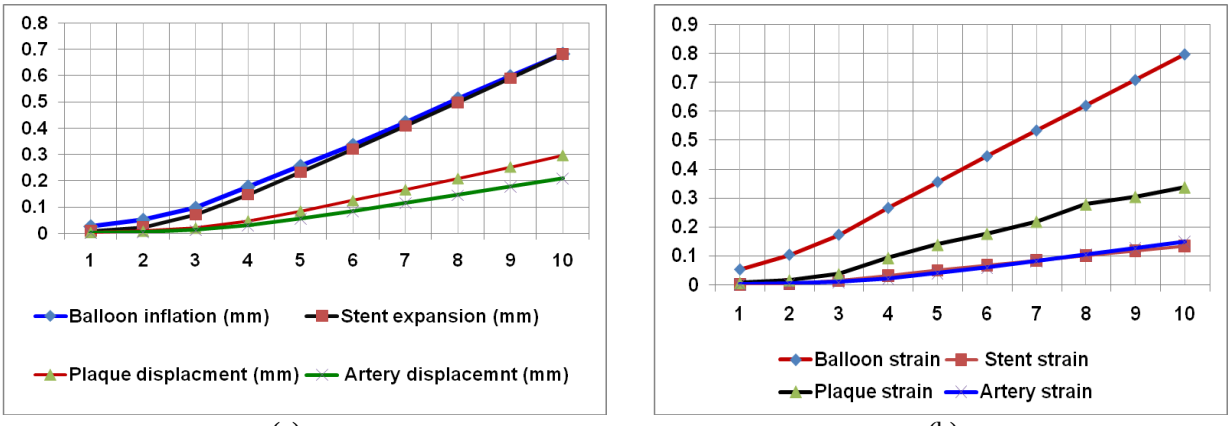


(a) (b)

Figure 2. Comparison of effect of incremental Pressure (on X-axis in atmosphere) on the variations of (a) Radial displacements (on Y-axis in mm) of BSPA distal ends, (b) Von-Mises strains (on Y-axis) of BSPA

ISSN: 0976 - 2965
IJBET (2009), 1(1):30-36

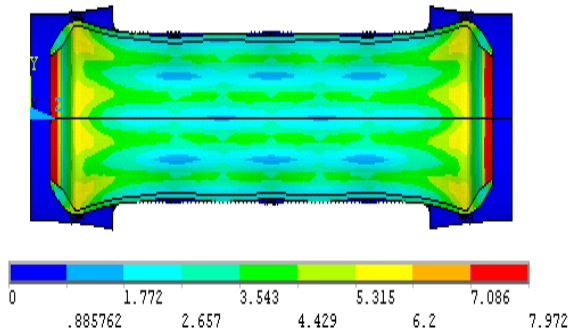


(a)

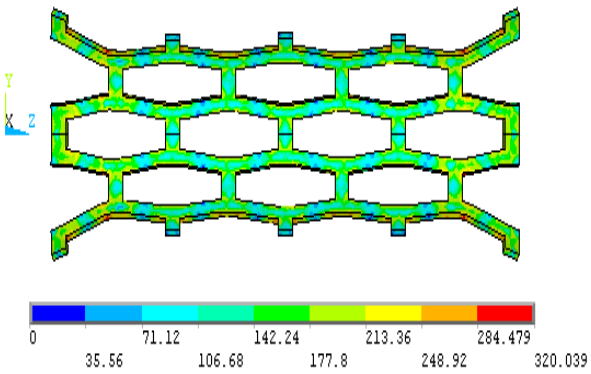


(b)

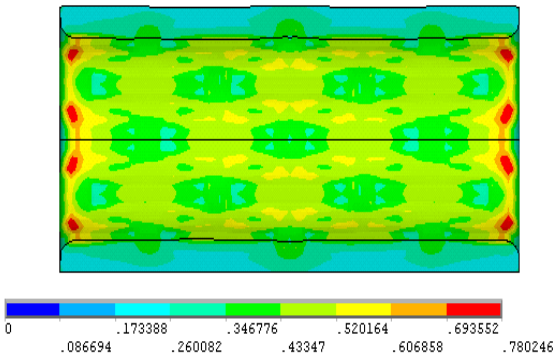


(c)

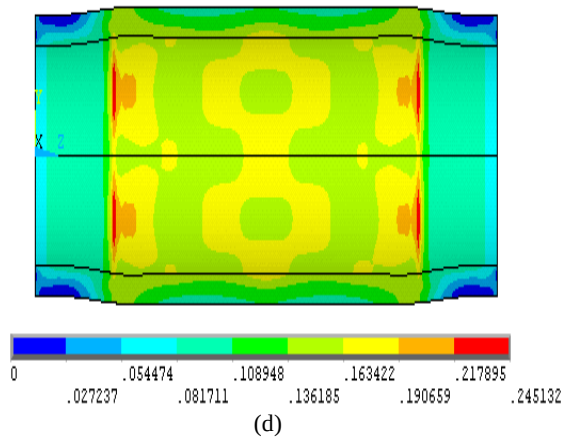


(d)

Figure. 3. Von-Mises stress distribution due to balloon inflation pressure of 1.0 MPa of (a) Balloon (b) Stent (c) Plaque (d) Artery

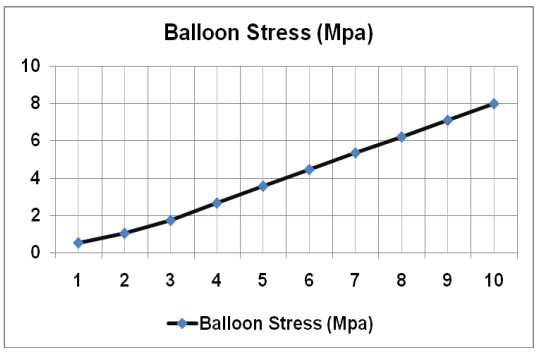


(a)

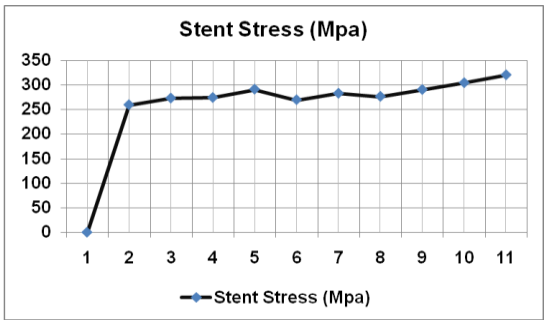


(b)

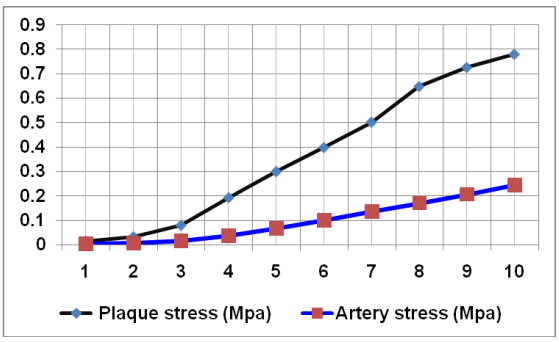


(c)

Figure. 4. Effect of incremental Pressure (on X-axis in atmosphere) on the variations of Von Mises Stresses in (a) Balloon, (b) in stent, (c) in plaque and artery (on Y-axis in MPa)

The highest compressive stresses in the radial direction are in the areas of contact between the stent struts and the arterial wall. The circumferential stresses show a considerable stress gradient from the internal to the external part of the arterial wall. The variation of Von-Mises stresses of each of BSPA system individually during stent deployment is shown graphically in Figure 4 (a-c) respectively. Though balloon is treated non-linear hyperelastic, the stresses observed to vary almost linearly Fig. 4 (a), therefore the same analysis using linear material properties Young's modulus 10 MPa and Poisson's ratio 0.45 was also carried out. The results of linear balloon were found to be almost same with $\pm$ 4% variation. Therefore it is suggested that to avoid the complexities and time consuming analyses one can consider linear balloon.

ISSN: 0976 - 2965
IJBET (2009), 1(1):30-36

As the pressure increases, the reaction force of the stent is no longer able to hold the balloon back to its original state. During the inflation process the proximal and distal ends of the expanding balloon, inflates first and causes the overlying stent to open non-uniformly into dogbonning. The centre of the slotted tube stent opened with increasing pressure and causes a contraction along its longitudinal axis (foreshortening). The expanding and sliding stent presses against the hard tissue (plaque) and plaque against the soft tissue (arterial wall). The nature of Von-Mises stresses on plaque and artery can be verified from Figure 4 (c). One of the nodes (Node Number-23010) located near the distal end of the stent and closest to plaque ends is observed to be responsible for tissue penetration causing the vascular injury.


(a)

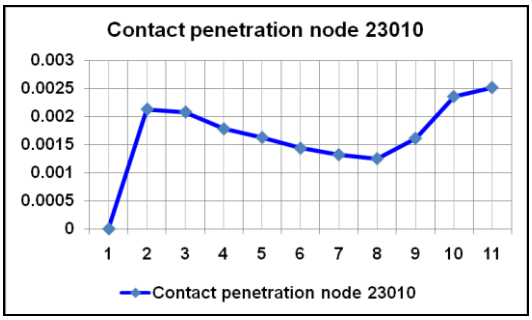


(b)

Figure. 5. (a) Location of Injury on Plaque
(b) Penetration of Node 23010 causing injury
(On Y-axis in mm).

The penetration of stent into the plaque tissue gives rise to high contact stresses of order 6.53 MPa damaging the blood vessel. The location of possible vascular injury caused b node 23010 is shown in shown in Figure 5 (a). Node 23010 is found to be on stent material. The variation of penetration of Node Number-23010 is shown in Fig. 5 (b). It is observed that the stent actually penetrates by about 0.003 mm inside the plaque. The contact penetration, contact stress and contact area are functions of placement pressure, stent geometry, and material behaviour of BSPA. These parameters help to develop a novel stent designs and stent-deployment protocols so as to minimize vascular injury and optimizing long-term outcomes.

## CONCLUSION

It is expected that the ultimate aim of all the studies related to stent deployment should remain to safeguard the vascular tissues (and not the implants) with maintained patency, however only a few researchers have incorporated the entire physics of Balloon-Stent-Plaque-Artery (BSPA) system. The interplay of BSPA should be considered more when we desire to design a less injurious stent delivery system, and thereby to obtain a high rate of success in stent implantation. The study demonstrates and partially quantifies the vascular injury and its likely locations and the extent. These results are promising and useful in the study of the mechanical performances of the entire BSPA system. In particular, they pointed out the possibility to optimize the radial expansion of the nonlinear behaviour of Balloon and stent in particular. The investigation provides the methodology for biomechanical characteristic of the vascular stent deployment procedure in a treatment of stenotic blood vessels. The appropriate geometric & material models, boundary conditions set and loading conditions for the numerical model allowed reflecting the phenomena occurring in the real object during implantation. Furthermore, the information obtained from the modeling considerations is very useful with respect to the optimization of the geometrical and material features of stents. It also can be used to predict a stability of the effective features of this type of implants. The acute contact of stent struts (and not the balloon) with plaque (and not the artery wall) has direct impact on vascular injury. The results of the investigation are in good agreement with available but limited previous studies. Therefore non-linear contact stress analysis of the mechanical and interactive behaviour of the Balloon-Stent-Plaque and Artery collectively is decisive for the design and application of similar vascular implants.

## ACKNOWLEDGEMENT

The authors thank Dr. H.M. Mardikar (Director *Spandan* Heart Institute and Research Center, Nagpur) & Dr. S. K. Deshpande (Sr. Radiologist CIMMS Hospital and Research center, Nagpur) for useful discussions, critical reviews, result approvals and validations of this work.
Authors are grateful to Dr. S. S. Gokhale, Director VNIT, for his kind and generous support towards the study.
The first author acknowledges Prof. S. N. Nakhare (V.J.T.I., Mumbai) and Prof. V. D. Raul (S.P.C.E., Mumbai) for consistent guidance, encouragement and developing multidisciplinary competency skills of author.

**REFERENCES**

[1] Lederman R., Mendelsohn F., Santos R., Phillips H., Stack R., Crowley J. (2001). Primary renal artery stenting: characteristics and outcomes after 363 procedures. American Heart Journal, 142:314-323.

[2] Mitra A.K. and Agrawal D.K. (2006). In stent restenosis: bane of the stent era. Journal of Clinical Pathology 59:232–239.

[3] Edelman E.R. and Rogers C. (1998) Pathobiologic responses to stenting. American Journal of Cardiology, 81:4E–6E.

[4] Schwartz, R. and Holmes, D.R. Pigs, dogs, baboons, and man; lessons in stenting from animal studies. Journal of Interventional Cardiology 7, 1994, 355–368.

[5] Kornowski R., Hong M.K., Tio F.O., Bramwell O., Wu H., Leon M.B. (1998) In-stent restenosis: contributions of inflammatory responses and arterial injury to neointimal hyperplasia. Journal of American College of Cardiology, 31:224–230.

[6] Harnek J., Zoucas E., Stenram U., Cwikiel W. (2002) Insertion of self-expandable Nitinol stents without previous balloon angioplasty reduces restenosis compared with PTA prior to stenting. Cardiovascular and Interventional Radiology, 25:430–436.

[7] Schiele F., Vuillemenot A., Meneveau N., Pales-Espinosa D., Gupta S., Bassand J.P. (1999) Effects of Increasing Balloon Pressure on Mechanism and Results of Balloon Angioplasty for treatment of Restenosis after Palmaz-Schatz Stent Implantation: An Angiographic and Intravascular Ultrasound Study. Catheterization and Cardiovascular Interventions, 46:214-231.

[8] Mario C.D., Stankovic G. (2000) Low or High Pressure for Stent Deployment? Not Always 'In Medio Stat Virtus'. Catheterization and Cardiovascular Interventions, 50:402-405.

[9] Liu S. Q. and Goldman J. (2001) Role of blood shear stress in the regulation of vascular smooth muscle cell migration. IEEE Transactions on Biomedical Engineering, 48:474-483.

[10] Kastrati A., Mehilli J., Dirschinger J., Pache J., Ulm K., Schulen H., Seyfarth M., Schmitt C., Blasini R., Neumann F.J., Schomig A. (2001) Restenosis after coronary placement of various stent types. American Journal of Cardiology, 87:34–39.

[11] Schwartz R.S. (1998) Pathophysiology of restenosis: interaction of thrombosis, hyperplasia, and/or remodeling. American Journal of Cardiology, 81:14E–17E.

[12] Lohavanichbutr K., Webb J.G., Carere R.G., Solankhi N., Jarochowski M., D'yachkova Y., Dodek A. (1999) Mechanisms, management, andoutcome of failure of delivery of coronary stents. American Journal of Cardiology, 83, 779-781.

[13] Morice M.C., Serruys P.W., Sousa J.E., Fajadet,J., BanHayashi E., Perin M., Colombo A., Schuler G., Barragan P., Guagliumi G., Molnar F., Falotico R. (2002) A randomized comparison of a sirolimus-eluting stent with a standard stent for coronary revascularization. New England Journal of Medicine, 346:1773-1780.

[14] Holzapfel G.A., Stadler M., Schulze-Bauer C.A. (2002) A layer-specific three-dimensional model for the simulation of balloon angioplasty using magnetic resonance imaging and mechanical testing. Annals of Biomedical Engineering, 30:753-767.

[15] Prendergast P.J., Lally C., Daly S., Reid A.J., Lee T.C., Quinn D., Dolan F. (2003) Analysis of prolapse in cardiovascular stents: a constitutive equation for vascular tissue and finite-element modelling. Journal of Biomechanical Engineering, 125:692-699.

[16] Lally C., Dolan F., Prendergast P.J. (2005) cardiovascular stent design and vessel stresses: a finite element analysis. Journal of Biomechanics, 38:1574-1581.

[17] Wang W.Q., Liang D.K., Yang D.Z., Qi M. (2006) Analysis of the transient expansion behavior and design optimization of coronary stents by finite element method. Journal of Biomechanics, 39:21–32.

[18] Takashima K., Kitou T., Mori K., Ikeuchi K. (2007) Simulation and experimental observation of contact conditions between stents and artery models. Medical Engineering and Physics, 29, 2007, 326–335.

[19] Dumoulin C., Cochelin B. (2000) Mechanical behaviour modelling of Balloon-expandable stents. Journal of Biomechanics, 33:1461-1470.

[20] Migliavacca F., Petrini L., Colombo M., Auricchio F., Pietrabissa R. (2002) Mechanical behavior of coronary stents investigated through the finite element method. Journal of Biomechanics, 35: 803-811.

[21] Migliavacca F., Petrini L., Montanari V., Quagliana I., Auricchio F., Dubini G. (2005) A predictive study of the mechanical behaviour of coronary stents by computer modelling. Medical Engineering and Physics, 27:13-18.Taylor J.G. (2002) Paying attention to consciousness. Trends in Cognitive Sciences 6(5):206-210

[22] Auricchio F., Di Loreto M., Sacco E. (2001) Finite-element analysis of a stenotic artery revascularization through a stent insertion. Computer Methods in Biomechanics and Biomedical Engineering, 4:249-263.

[23] Gu L., Santra S., Mericle R.A., Kumar A.V. (2005) Finite element analysis of covered microstents. Journal of Biomechanics, 38:1221–1227.

[24] Gervaso F., Capelli C., Petrini L., Lattanzio S., Di Virgilio L., Migliavacca F. (2008) On the effects of different strategies in modelling balloon-expandable stenting by means of finite element method. Journal of Biomechanics, 41:1206-1212.

[25] Raamachandran J., Jayavenkateshwaran K. (2007) Modeling of stents exhibiting negative Poisson's ratio effect. Computer Methods in Biomechanics and Biomedical Engineering, 10:245-255.